Cancer Cell
Article

Targeting Nonclassical Oncogenes for Therapy in T-ALL

Prem S. Subramaniam,[1] Dosh W. Whye,[1] Evgeni Efimenko,[1] Jianchung Chen,[1] Valeria Tosello,[3] Kim De Keersmaecker,[3] Adam Kashishian,[4,5] Mary Ann Thompson,[6] Mireia Castillo,[8] Carlos Cordon-Cardo,[8] Utpal P. Davé,[7] Adolfo Ferrando,[1,2,3] Brian J. Lannutti,[4,5] and Thomas G. Diacovo[1,2,*]
[1]Department of Pediatrics
[2]Department of Pathology and Cell Biology
Columbia University Medical Center, New York, NY 10032, USA
[3]Institute for Cancer Genetics, Columbia University, New York, NY 10032, USA
[4]Calistoga Pharmaceuticals, Seattle, WA 9810, USA
[5]Gilead Sciences, Seattle, WA 9810, USA
[6]Department of Pathology
[7]Department of Medicine and Cancer Biology
Vanderbilt University Medical Center, Nashville, TN 37232, USA
[8]Department of Genetics and Genomic Sciences, The Mount Sinai School of Medicine, New York, NY 10029, USA
*Correspondence: td2142@columbia.edu
DOI 10.1016/j.ccr.2012.02.029

SUMMARY

Constitutive phosphoinositide 3-kinase (PI3K)/Akt activation is common in T cell acute lymphoblastic leukemia (T-ALL). Although four distinct class I PI3K isoforms (α, β, γ, δ) could participate in T-ALL pathogenesis, none has been implicated in this process. We report that in the absence of PTEN phosphatase tumor suppressor function, PI3Kγ or PI3Kδ alone can support leukemogenesis, whereas inactivation of both isoforms suppressed tumor formation. The reliance of PTEN null T-ALL on the combined activities of PI3Kγ/δ was further demonstrated by the ability of a dual inhibitor to reduce disease burden and prolong survival in mice as well as prevent proliferation and promote activation of proapoptotic pathways in human tumors. These results support combined inhibition of PI3Kγ/δ as therapy for T-ALL.

INTRODUCTION

Constitutive activation of the phosphoinositide 3-kinase (PI3K)/Akt signal transduction pathway is a common event in cancer, promoting the growth, proliferation, and survival of various types of tumors including T cell acute lymphoblastic leukemia (T-ALL) (Yuan and Cantley, 2008; Zhao and Vogt, 2008; Gutierrez et al., 2009; Palomero et al., 2008; Silva et al., 2008; Larson Gedman et al., 2009). Class I PI3Ks are a family of lipid kinases that generate the potent second messenger phosphatidylinositol-3,4,5 trisphosphate (PIP_3) in response to ligation of a number of distinct cell surface receptors (Katso et al., 2001; Cantley, 2002). This results in the activation of Akt as well as numerous downstream effector molecules, which ultimately promote cell growth and survival. Class I PI3Ks are heterodimeric molecules composed of a regulatory and a catalytic subunit, the latter consisting of four unique isoforms that include p110α, p110β, p110γ, and p110δ. Each is capable of regulating distinct biological functions in normal tissues and cellular compartments. However, some overlap in activity does exist, as is the case for thymocytes where the combined activities of PI3Kγ and PI3Kδ contribute to cellular processes required for the generation and function of mature T cells (Webb et al., 2005; Swat et al., 2006; Ji et al., 2007). Although the importance of these two PI3K isoforms in T cell biology is well established (Okkenhaug and Vanhaesebroeck, 2003), what role, if any, they

Significance

Loss of PTEN function is a frequent occurrence in cancer resulting in unbridled PI3K/Akt signaling that contributes to tumor pathogenesis. Consequently, much emphasis has been placed on developing inhibitors that target this pathway. Here, we report that PI3Kγ and PI3Kδ act as a tumorigenic bottleneck in PTEN null T-ALL. We also demonstrate that it is possible to exploit the "addiction" of a hematological malignancy to specific PI3K isoforms, enabling the rational design of a PI3Kγ/δ dual inhibitor. This work represents a significant advancement in our understanding of the dynamic interplay that exists between PTEN and particular PI3K isoforms in regulating both normal and abnormal T cell development as well as in sustaining tumor cell proliferation and survival.

play in malignant transformation and tumor cell survival remains to be determined.

Previously, it has been reported that p110α is involved in oncogenesis because function-enhancing mutations in this catalytic subunit are found in many cancers of solid organs (Samuels et al., 2004; Zunder et al., 2008). In contrast, cancer-specific mutations have yet to be identified for the other p110 isoforms. That said, overexpression of p110β, p110γ, or p110δ in an in vitro culture system induces cellular transformation (Kang et al., 2006). Moreover, increased or preferential expression of p110γ and p110δ has been described in chronic and acute forms of myeloid leukemia, respectively (Hickey and Cotter, 2006; Sujobert et al., 2005). However, to our knowledge, overexpression of specific PI3K isoforms has not been reported for T-ALL, and mutations in PI3Kα are rare, suggesting that they are not a major contributor to its pathogenesis (Gutierrez et al., 2009; Lo et al., 2009).

PTEN is a nonredundant plasma-membrane phosphatase that is responsible for counteracting the potential cancer-promoting activities of class I PI3K (Sulis and Parsons, 2003; Salmena et al., 2008). It does so by limiting the levels of PIP_3 generated in response to the activation of these lipid kinases. Clinically, mutations in the *PTEN* tumor suppressor gene are common in multiple types of human cancer, resulting in unbridled PI3K/Akt signaling as well as conferring resistance to chemotherapeutic agents (Carnero et al., 2008; Huang and Hung, 2009). It has been well established that deletion of the tumor suppressor gene *PTEN* in T cell progenitors drives the malignant transformation of these cells within the thymus of mice (Suzuki et al., 2001; Hagenbeek and Spits, 2008; Liu et al., 2010). Moreover, the resulting tumors possess similar genetic and biochemical aberrations associated with a subset of patients with T-ALL including hyperactivation of the PI3K/Akt signaling pathway (Maser et al., 2007; Guo et al., 2008). In fact Gutierrez et al. (2009) have reported a loss of PTEN function due to mutations or deletions in approximately 40% of primary T-ALL samples, suggesting that hyperactivation of the PI3K/Akt signaling pathway is a common feature of this hematological malignancy. Based on these clinical observations and known reliance of thymocyte development on PI3Kγ and PI3Kδ, we set out to determine whether these nonclassical oncogenes contribute to leukemogenesis and if it is possible to exploit tumor cell "addiction" to the activity of distinct PI3K isoforms, thus permitting the rational design of a chemotherapeutic agent to treat T-ALL.

RESULTS

PI3Kγ or PI3Kδ Can Support Malignant Transformation of T Cells

We crossed mice containing both *Pten* alleles floxed by the loxP Cre excision sites with *Lck*-cre transgenic animals (*Lck/Pten*$^{fl/fl}$) alone or together with those lacking p110γ, encoded by *Pik3cg*, and/or p110δ, encoded by *Pik3cd*, catalytic subunits. Consistent with previous studies, >85% of *Lck/Pten*$^{fl/fl}$ mice develop T-ALL and eventually succumb to the disease (median survival of 140 days), which was confirmed by flow cytometric analysis (Figures 1A and 1B). In contrast to PTEN null tumors of solid organs that have been reported to rely on PI3Kβ activity (Jia et al., 2008; Wee et al., 2008), tumorigenesis in the context of a deficiency of PTEN in T cell progenitors appears to be critically dependent on PI3Kγ and PI3Kδ. This is evidenced by the marked delay in the onset of disease and increased survival of *Lck/Pten*$^{fl/fl}$*;Pik3cg*$^{-/-}$*;Pik3cd*$^{-/-}$ triple-mutant mice (TKO) because <20% of animals succumb to T-ALL by 220 days. However, the activity of either isoform alone was sufficient to promote tumor formation, yielding similar median survival times for *Lck/Pten*$^{fl/fl}$*;Pik3cg*$^{-/-}$ and *Lck/Pten*$^{fl/fl}$*;Pik3cd*$^{-/-}$ mice (175 versus 178 days, respectively). Comparable percentages of these animals developed and died of T-ALL (65% versus 64%, respectively), and tumors had evidence of activation of the PI3K/Akt signaling pathway, albeit much reduced as compared to those from *Lck/Pten*$^{fl/fl}$ animals (Figure 1C). However, there was no evidence of overexpression of any *Pik3c* isoform in thymic tumors (Figure 1D).

Further evidence demonstrating that it is the unleashed activities of PI3Kγ and PI3Kδ that provide the signals necessary for the development of T-ALL is suggested by the continued reduction in thymus size and cellularity in 6-week-old TKO mice (Figure 2A). Although absence of PTEN should permit unrestricted activity of all four class I PI3K isoforms, it appears that PI3Kα and PI3Kβ cannot adequately compensate for their γ and δ counterparts as evidenced by the persistent diminution in the total number of $CD4^+CD8^+$ double-positive thymocyte population and near-basal levels of phosphorylated Akt (Ser473) as compared to mice deficient in PTEN alone (Figures 2A and 2B). Cellular alterations associated with p110γ/δ double deficiency also persisted in the peripheral blood and in secondary lymphoid organs of TKO mice and included a paucity of $CD3^+$ T cells (Figures 2C and 2D). No active tumor was found in peripheral blood or spleen of the surviving animals at ~7 months of age as determine by absence of staining for the proliferation marker Ki67 on Thy1.2-positive cells (Figure 2E).

Effect of PI3Kγ/PI3Kδ Dual Inhibition on Thymocyte Signaling and Development

In order to ascertain whether PI3Kγ and PI3Kδ are also required for tumor maintenance and can be targeted therapeutically in T-ALL, we generated a small molecule that preferentially inhibits the function of both p110γ and p110δ catalytic domains, designated CAL-130 (Figure 3A). IC_{50} values of this compound were 1.3 and 6.1 nM for p110δ and p110γ, respectively, as compared to 115 and 56 nM for p110α and p110β. Importantly, this small molecule does not inhibit additional intracellular signaling pathways (i.e., p38 mitogen-activated protein kinase or insulin receptor tyrosine kinase) that are critical for general cell function and survival (Table 1; see Table S1 available online). To demonstrate that CAL-130 can block the activities of both PI3Kδ and PI3Kγ in thymocytes, we evaluated its ability to prevent phosphorylation of Akt (Ser473) and calcium flux in response to T cell receptor (TCR) crosslinking. Previously, we have shown that the combined activities of these two class I PI3K isoforms are necessary for phosphorylation of this protein kinase in this cell population (Swat et al., 2006). Consistent with these results, CAL-130 treatment of thymocytes harvested from 6-week-old WT animals prevented TCR-induced Akt phosphorylation and attenuated calcium flux to levels observed for their *Pik3cg*$^{-/-}$*;Pik3cd*$^{-/-}$ counterparts (Figures 3B, 3C, and S1A).

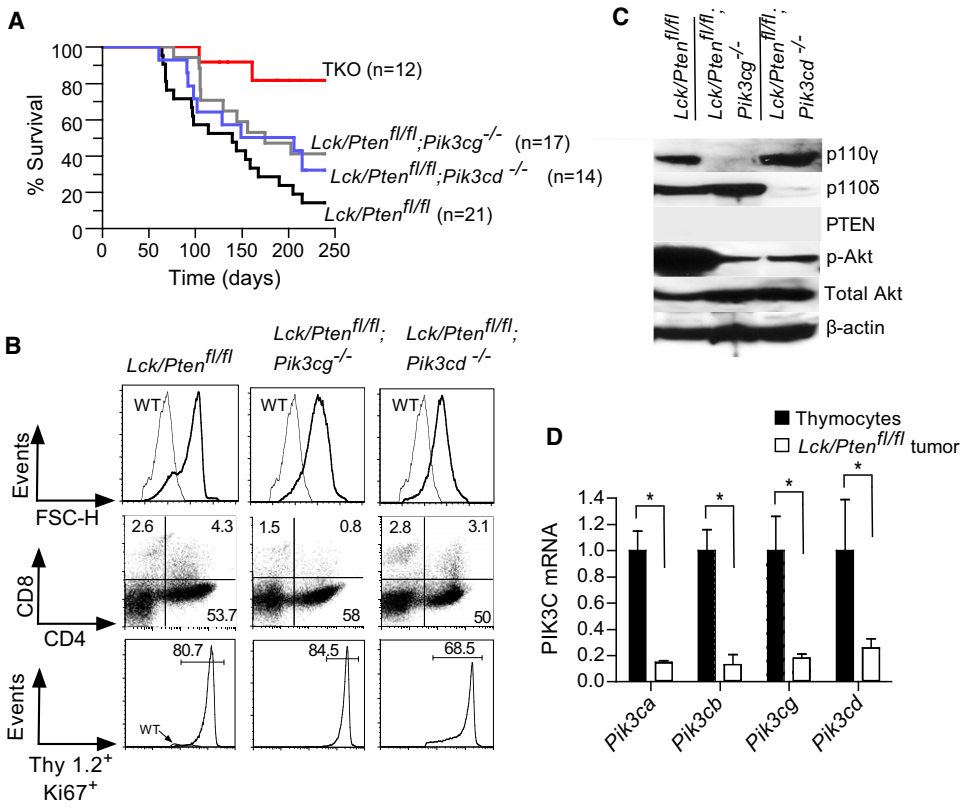

Figure 1. PI3Kγ or PI3Kδ Can Support Leukemogenesis in the Context of PTEN Deficiency

(A) Kaplan-Meyer survival curves demonstrating the requirement for PI3Kγ and PI3Kδ activity in the development of PTEN null T-ALL. All animals were followed for a period of 7 months.

(B) Representative flow cytometric profiles of peripheral blood from diseased mice lacking p110γ or p110δ in the absence of PTEN in T cell progenitors. Forward scatter (FSC) and Ki67 staining are indicators of cell size and proliferation, respectively. Thy 1.2 expression identifies T-lineage cells.

(C) Representative immunoblots depicting p110γ, p110δ, and PTEN expression as well as Akt activation state (phosphorylation of Ser473) in thymic lysates from the same animals.

(D) Quantitative reverse-transcription PCR analysis of *Pik3c (a/b/g/d)* transcript levels in WT thymocytes (n = 5) and tumors (n = 5) harvested from *Lck/Pten*$^{fl/fl}$ mice. Error bars represent ±SD. The difference in *Pik2c* expression levels between the WT thymocytes and tumor cells was statistically significant (*$p < 0.05$) using a Student's t test.

To assess the in vivo efficacy of the inhibitor, we determined its effects on thymi of 6-week-old WT mice, specifically for its ability to recapitulate the phenotype observed when both p110γ and p110δ are deficient. Animals received 10 mg kg^{-1} of the inhibitor orally, which was sufficient to maintain plasma concentrations of 0.33 ± 0.18 μM at the end of 8 hr (Figure 3D). Notably, this dose did not affect either plasma glucose or insulin levels in contrast to the metabolic perturbations associated with tissue-specific deficiencies in p110α and p110β (Figures 3E and 3F) (Jia et al., 2008; Sopasakis et al., 2010). CAL-130 was also found to have a limited ability to impair PDGF-induced activation of PI3Kα as compared to the pan-PI3K/mTOR inhibitor BEZ235 (Figure S1B). Similarly, platelets harvested from *Pik3cg*$^{-/-}$*;Pik3cd*$^{-/-}$ mice 2 hr post-administration of CAL-130 had no obvious defect in ADP-mediated platelet aggregation, a process known to rely predominantly on PI3Kβ (Figure S1C) (Jackson et al., 2005). However, CAL-130 treatment (10 mg kg^{-1} every 8 hr) for a period of 7 days markedly affected the size, cellularity, and overall architecture of the thymus faithfully reproducing the phenotype associated with *Pik3cg*$^{-/-}$*;Pik3cd*$^{-/-}$ mice (Figure 3G). In particular there was a 18-fold reduction in total thymocyte number in comparison to controls, which was primarily due to the loss of DP population (Figure 3H). These observations are consistent with the ability of CAL-130 to preferentially block the function of both PI3Kγ and PI3Kδ.

Antileukemic Effects of Pharmacological Inhibition of PI3Kγ and PI3Kδ in PTEN Null T-ALL Tumors in Mice

The clinical significance of interfering with the combined activities of PI3Kγ and PI3Kδ was determined by administering CAL-130 to *Lck/Pten*$^{fl/fl}$ mice with established T-ALL. Candidate animals for survival studies were ill appearing, had a white blood cell (WBC) count above 45,000 μl^{-1}, evidence of blasts on peripheral smear, and a majority of circulation cells (>75%) staining double positive for Thy1.2 and Ki-67. Mice received an oral dose (10 mg kg^{-1}) of the inhibitor every 8 hr for a period of 7 days and were then followed until moribund. Despite the limited duration of therapy, CAL-130 was highly effective in extending the median survival for treated animals to 45 days as compared 7.5 days for the control group (Figure 4A).

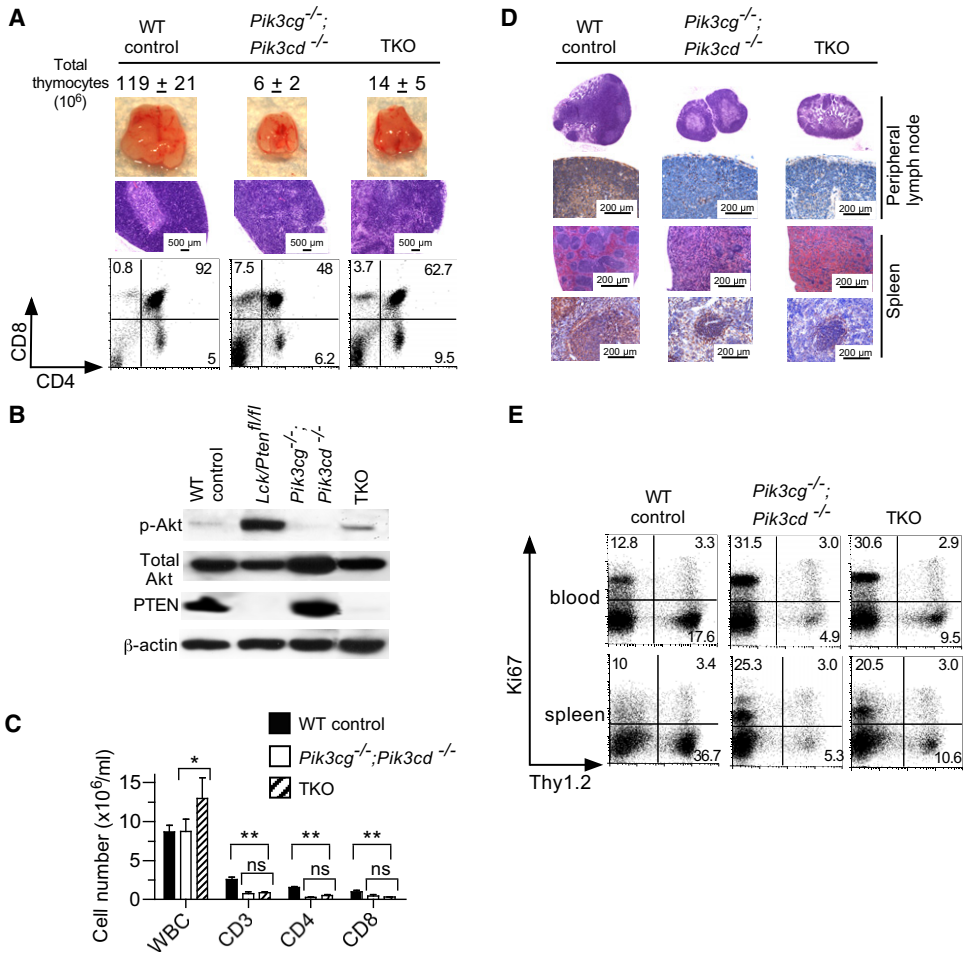

Figure 2. Persistence of Cellular and Structural Defects in Thymi Associated with a Combined Deletion of p110γ/p110δ and PTEN

(A) Hematoxylin and eosin staining (H&E) and flow cytometric analyses of thymi derived from 6-week-old mice lacking both p110γ and p110δ catalytic subunits in the presence or absence of PTEN. The panels are representative of data from five animals in each group.

(B) Immunoblots assessing for Akt phosphorylation (Ser473) and PTEN levels in thymocyte lysates.

(C) Number of WBC and T cell subsets in the peripheral blood of the same animals. *ns (not significant) for *Pik3cg*$^{-/-}$;*Pik3cd*$^{-/-}$ versus TKO; **$p < 0.01$ for WT versus TKO.

(D and E) Representative (D) micrografts of H&E peripheral lymph nodes and spleen and (E) flow cytometry plots of blood and spleen from triple mutant animals (n = 5 mice per genotype). Histological identification of T cells was by immunoperoxidase detection of CD3. Scale bars correspond to 200 μm in secondary lymphoid organs and to 500 μm in thymi. Data represent the mean ± SD.

To determine the effect of CAL-130 on disease burden, we performed sequential blood counts and peripheral smears as well as flow cytometric analyses on *Lck/Pten*$^{fl/fl}$ mice pre- and post-administration of the inhibitor (Figures 4B and S2A–S2C). All animals showed a dramatic reduction in WBC count by day 4 reflected in the loss of the highly proliferative blast population (Thy1.2/Ki-67 double positive, high FSC-H), which remained at low levels for the duration of treatment. Moreover, both CD4 single-positive and CD4/CD8 double-positive T-ALL responded to CAL-130, which corresponded with an increase in apoptosis detected as sub-G0 population after propidium iodide (PI) staining on days 4–7. Treatment of diseased *Lck/Pten*$^{fl/fl}$;*Pik3cg*$^{-/-}$ mice but not their *Lck/Pten*$^{fl/fl}$ counterparts with the PI3Kδ selective inhibitor IC87114 (10 mg kg^{-1} every 8 hr) produced similar results, confirming the critical reliance of PTEN null tumors on the combined activities of PI3Kγ and PI3Kδ (Figures 4C and S2D).

Further evidence to support the ability of CAL-130 to reduce tumor burden was obtained by bioluminescent imaging. *Pten*$^{fl/fl}$ mice were crossed with a strain in which a luciferase cDNA, preceded by a LoxP-stop-LoxP cassette, was introduced into the ubiquitously expressed *ROSA26* locus (Safran et al., 2003). Progenies were then crossed with *Lck*-cre transgenics to delete *Pten* in T cell progenitors and induce expression of luciferase (*Lck/Pten*$^{fl/fl}$;*Gt(ROSA)26Sor*$^{tm1(Luc)Kael}$/J). Imaging of T-ALL tumor-bearing animals was performed just prior to and after 4 days of treatment with CAL-130. Signals at day 4 were dramatically lower in treated animals, consistent with the reduction in the WBC count and the CD4 single-positive population of tumor cells (Figure 4D). Moreover, weights of thymi, liver, spleen, and kidneys from treated *Pten*$^{fl/fl}$ mice were significantly less than that for animals that received vehicle control for 7 days (Figure 4E).

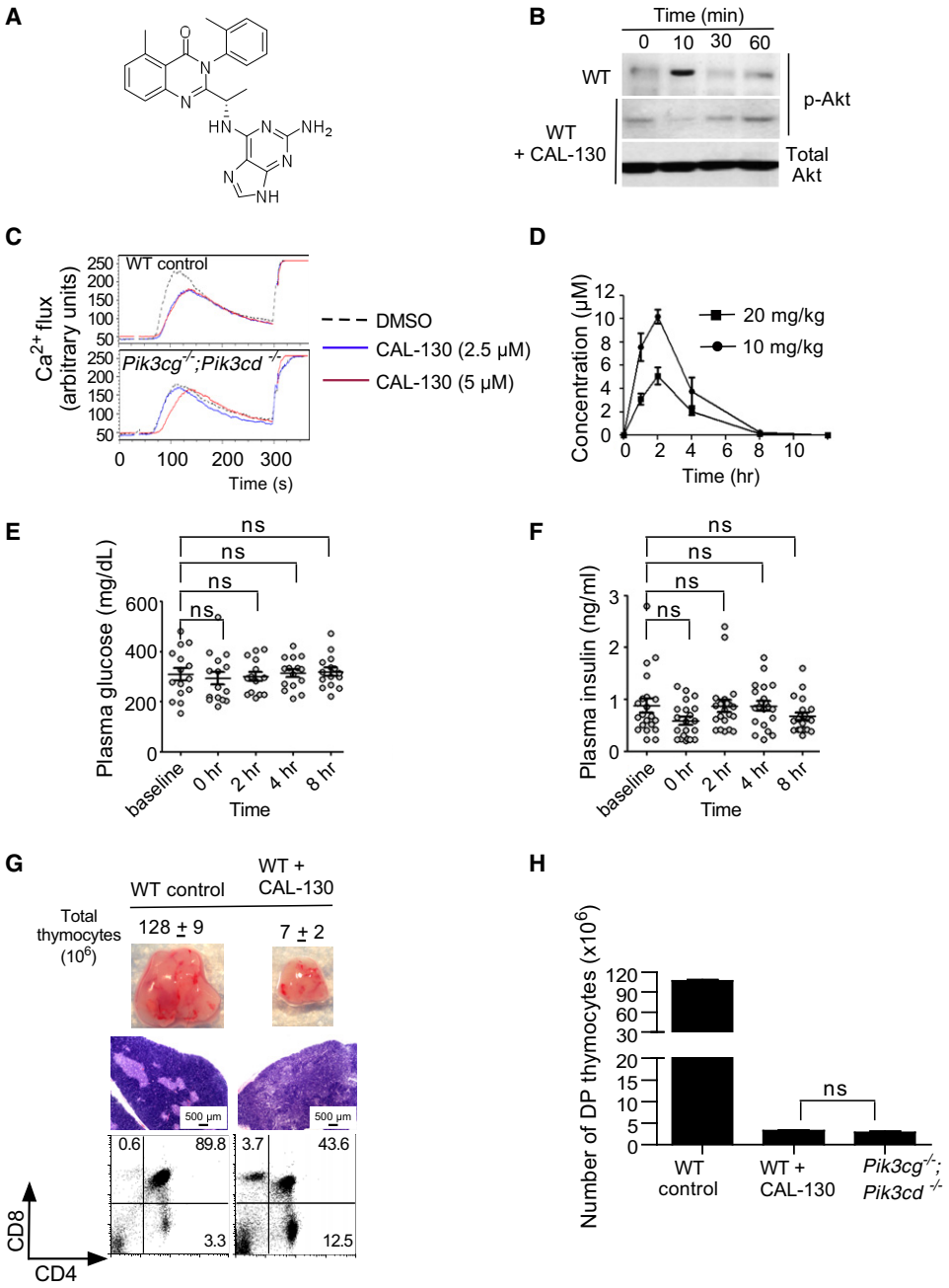

Figure 3. Inhibitory Profile of CAL-130

(A) Chemical structure of CAL-130.

(B and C) Effect of the inhibitor on (B) Akt phosphorylation (Ser473) or (C) Ca^{2+} flux in purified thymocytes from WT or *Pik3cg*$^{-/-}$;*Pik3cd*$^{-/-}$ animals in response to TCR crosslinking. Data are representative of three separate experiments.

(D) Plasma concentrations of CAL-130 in mice after a single oral dose (n = 4).

(E and F) Plasma glucose (E) and corresponding insulin levels (F) in WT mice before and after receiving a single dose of inhibitor (10 mg kg^{-1}). $p > 0.5$ for glucose and $p > 0.2$ for insulin as compared to baseline (n = 15 mice per time point; ns, not significant).

(G) Phenotypic analyses of thymi from mice treated with either CAL-130 (10 mg kg^{-1} every 8 hr) or vehicle control for 7 days. The panels are representative of data from five animals in each group.

(H) Total DP thymocyte count in the same animals in (G). Results are compared to PI3Kγ/δ double-knockout mice. Data represent the mean ± SD.

See also Figure S1.

Table 1. P110 Catalytic Domain Selectivity of CAL-130 as Assessed by Ambit KinomeScan Screening

Ambit Gene Symbol	Control Binding (%)	Ambit Gene Symbol	Control Binding (%)
PIK3CA	12	PIK3CG	3.2
PIK3CB	10	PIK3CD	0.2

CAL-130 (10 μM) was evaluated for its ability to prevent tagged kinases from interacting with immobilized "bait" ligand (Fabian et al., 2005; Karaman et al., 2008). Results are reported as percentage (%) of control binding, where lower numbers indicate stronger interactions with the tagged kinase. Values >35% are considered "no hits." PI3Kδ had the lowest percentage of control binding at 0.2% followed by PI3Kγ at 3.2%, indicating a high probability of a potent interaction. A total of 353 kinases were assessed in the screen (Table S1).

Reliance of PTEN Null Human T-ALL on PI3Kγ and PI3Kδ

To test whether CAL-130 may have similar effects on human tumors, we first analyzed the response of T-ALL cell lines to the compound. Incubation of cultured cells with CAL-130, but not inhibitors of either PI3Kγ or PI3Kδ, prevented proliferation and promoted apoptosis within 24 hr, which persisted over 4 days of treatment (Figures 5A, 5B, and S3A–S3J). To further demonstrate that the combined activities of PI3Kγ and PI3Kδ are essential for these processes, we utilized an shRNA vector that targeted the p110γ catalytic domain in CCRF-CEM cells. Western blot analysis revealed a >95% reduction in expression of p110γ with no effect on the other isoforms (Figure 5C, inset). Subsequent incubation of these cells with the PI3Kδ-specific inhibitor IC87114 prevented proliferation and promoted apoptosis as observed for nontransfected CCRF-CEM exposed to CAL-130 (Figures 5C and 5D). In contrast, IC87114 had no major effect on cells containing empty vector alone; neither did siRNA knockdown of either p110α or p110β (Figures S3K–S3N). These observations are consistent with our in vivo studies demonstrating that PI3Kγ and PI3Kδ are strictly required for the proliferation and survival of T-ALL lymphoblasts. Moreover, blockade of these two isoforms significantly enhanced the apoptotic properties of dexamethasone, a drug of considerable importance in the treatment of various lymphoid malignancies including T-ALL (Figures 5E–5H) (Beesley et al., 2009).

It is well known that PI3K/Akt signaling pathway can play a major role in cell-cycle progression and growth of tumors by regulating the activation state of the downstream targets such as glycogen synthase kinase-3β (GSK3β) and mTOR (Schmelzle and Hall, 2000; Cohen and Frame, 2001). PI3K/Akt-mediated phosphorylation suppresses the function of the former and promotes the activity of the latter. Tumor cell survival, on the other hand, is largely mediated by the ability of this pathway to inactivate proapoptotic effectors such as the BH3-only proapoptotic protein BAD and to repress the expression of BIM, both of which participate in the mitochondria-dependent cell death pathway (Strasser et al., 2000; Duronio, 2008). Therefore, we examined the ability of CAL-130 treatment to interfere with such events. Indeed, CCRF-CEM cells exposed to increasing concentration of drug exhibited a corresponding reduction and complete abrogation of Akt (Ser473) phosphorylation at 2.5 μM (Figure 6A). Downstream targets of this protein kinase were also affected as evidenced by the reduction in phosphorylation of GSK3β and mTOR. Consistent with the importance of PI3K in tumor cell survival, CAL-130 treatment resulted in a reduction in phosphorylation of BAD, as well as an enhanced expression of its counterpart BIM (including the L and S isoforms) (Figure 6B). The latter would also explain in part the synergy between CAL-130 and dexamethasone because BIM expression is required for glucocorticoid-induced apoptosis (Erlacher et al., 2005; Wang et al., 2003).

To assess the in vivo relevance of these observations, we evaluated the ability of CAL-130 to prevent the proliferation of CCRF-CEM cells implanted subcutaneously or to prolong the survival of NOD.Cg-*Prkdc*^{scid} *Il2rg*^{tm1Wjl}/Sz that received these cells intravenously. In the former, luciferase-expressing CCRF-CEM cells were injected into the flanks of immunodeficient mice and allowed to grow for 1 week before administering vehicle control or inhibitor (10 mg kg^{-1} every 8 hr) for a total of 4 days. In the latter, treatment commenced 3 days postinjection of tumor cells for a total of 7 days. Bioimaging of subcutaneous tumors revealed a 5-fold difference in luminescence in CAL-130-treated versus vehicle control-treated animals (Figure 6C). This translated into an increase in median survival time for treated animals with systemic disease of 35 versus 23 days for mice that received vehicle control alone (Figure 6D).

Because the continued passage of rapidly growing tumor lines can result in genetic alterations distinct from the cell from which it was originally derived, we also evaluated the effect of CAL-130 on primary T-ALL samples isolated from patients with active disease. Consistent with our animal studies, human tumor cells devoid of PTEN were exquisitely sensitive to dual inhibition of PI3Kγ/δ, but not single inhibition of PI3Kδ, which resulted in a reduction in tumor cell viability as well as in Akt phosphorylation in response to treatment (Figures 7A–7C; data not shown). Interestingly, one primary sample that not only expressed PTEN (T-ALL 4) but also high levels of phospho-Akt was as responsive to CAL-130 as its PTEN null counterparts. This would suggest that T-ALL sensitivity to a PI3Kγ/δ dual inhibitor might correlate better with the degree of Akt phosphorylation rather than with PTEN expression. As observed with primary mouse T-ALL, human tumors did not appear to overexpress any of the four class I *PIK3C* isoforms (Figure 7D).

DISCUSSION

Oncogenesis is a complex and multigenic process that often involves constitutive activation of the PI3K signaling pathway. Most notably are the gain-of-function mutations frequently found in *PIK3CA*, the gene that encodes for the p110α catalytic subunit, and genetic alterations that lead to the inactivation of the tumor suppressor gene *PTEN* (Samuels et al., 2004; Zunder et al., 2008; Sulis and Parsons, 2003; Salmena et al., 2008). In the latter scenario the possibility exists that the unregulated activity of any of the four class I PI3K isoforms could drive tumor development. For instance, previous reports demonstrate that PI3Kβ is essential for the induction, growth, and survival of PTEN-deficient tumors of epithelial cell origin (Jia et al., 2008; Wee et al., 2008). Moreover, it has been suggested that all class I PI3K isoforms are capable of coupling to upstream signaling pathways in which they are not normally engaged, thus compensating for inhibition/genetic deletion of a particular isoform

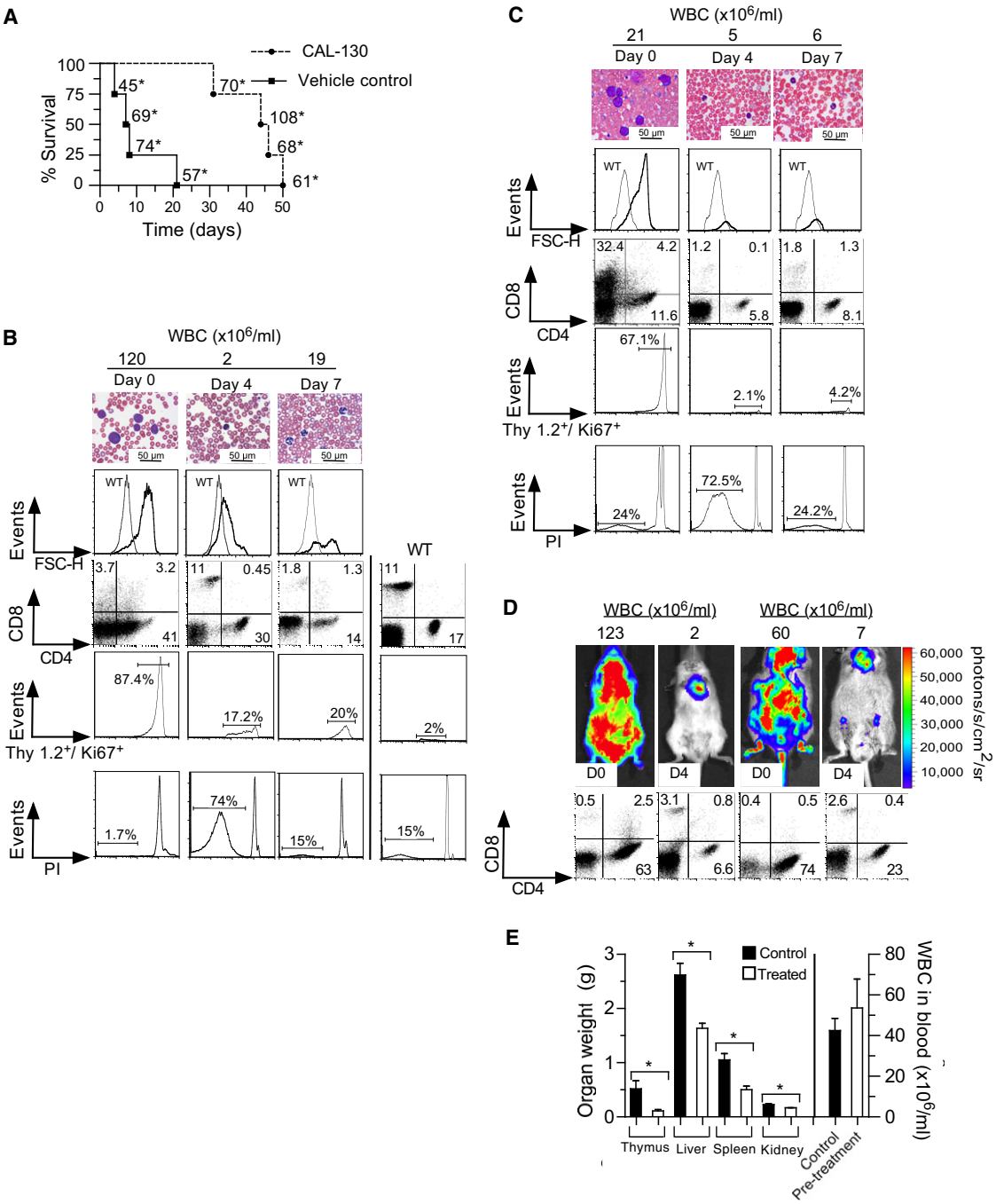

Figure 4. Combined Inhibition of p110γ and p110δ Reduces Tumor Burden and Increases Survival in Animals with PTEN Null T-ALL

(A) Kaplan-Meyer survival curve for *Lck/Pten*$^{fl/fl}$ mice diagnosed with T-ALL and immediately treated with CAL-130 for a total of 7 days. $p < 0.001$ for CAL-130 treated versus vehicle control. Numbers with an asterisk (*) represent the initial WBC count ($\times 10^6$) for each animal prior to instituting therapy.

(B and C) Peripheral blood smears and flow cytometric profiles for diseased (B) *Lck/Pten*$^{fl/fl}$ and (C) *Lck/Pten*$^{fl/fl}$;*Pik3cg*$^{-/-}$ mice just before and 4 and 7 days after initiating treatment with either CAL-130 or the PI3Kδ-specific inhibitor IC87114, respectively. The panels are representative of data from four *Lck/Pten*$^{fl/fl}$ mice and two *Lck/Pten*$^{fl/fl}$;*Pik3cg*$^{-/-}$ mice with T-ALL. Untreated WT animal is shown for comparison.

(D) Bioluminescent images and corresponding flow cytometric profiles of *Lck/Pten*$^{fl/fl}$/*Gt(ROSA)26Sor*$^{tm1(Luc)Kael}$/J animals with T-ALL immediately before and 4 days after treatment.

(E) Weights of thymi, liver, spleen, and kidneys harvested from *Lck/Pten*$^{fl/fl}$ mice with T-ALL 7 days posttreatment with either CAL-130 or vehicle control (n = 5, *$p < 0.01$ for CAL-130 treated versus vehicle control). Peripheral blood counts (WBC, right axis) represent the mean ± SD prior to treatment.

See also Figure S2.

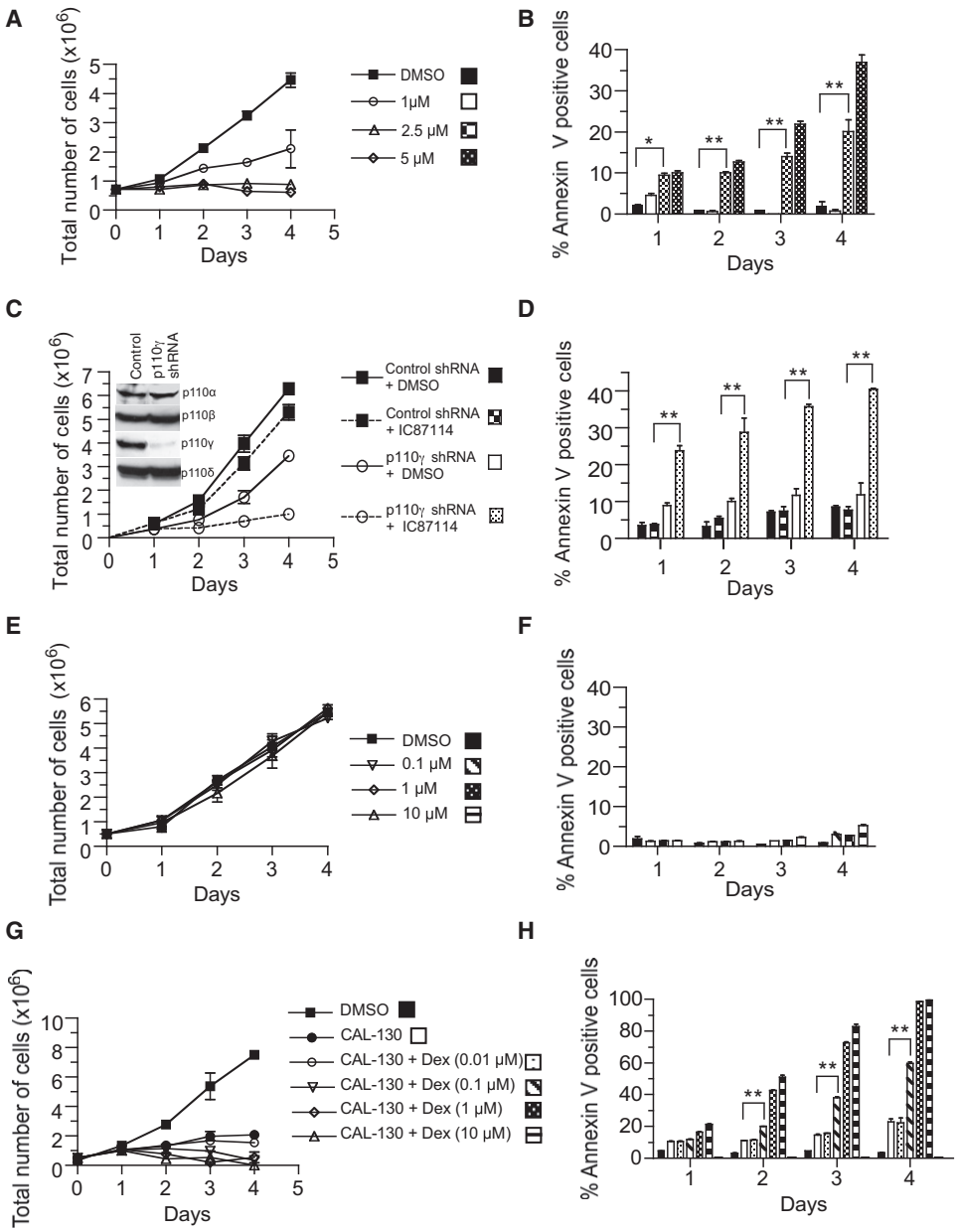

Figure 5. Contribution of PI3Kγ and PI3Kδ to the Growth and Survival of PTEN Null Human T-ALL Tumor Cell Lines

(A and B) Proliferation (A) and survival (B) of CCRF-CEM cells cultured in the presence of CAL-130 or vehicle control. *$p < 0.01$, **$p < 0.001$ for CAL-130 treated (2.5 μM) versus DMSO.

(C and D) Effect of the PI3Kδ-specific inhibitor IC87114 (10 μM) on proliferation (C) and survival (D) of CCRF-CEM cells in which p110γ expression was knocked down by shRNA transfection. **$p < 0.001$ for p110γ shRNA treated with IC87114 versus nonsilencing vector treated with IC87114. Inset in (C) depicts western blot analysis for p110 catalytic subunits.

(E–H) Proliferation and survival of CCRF-CEM cells cultured in the presence of dexamethasone alone (E and F) or in combination with 2.5 μM CAL-130 (G and H). **$p < 0.001$ for dexamethasone plus CAL-130 treated (2.5 μM) versus CAL-130 (2.5 μM) alone. Data represent the mean ± SD of experiments performed in triplicate.

See also Figure S3.

(Foukas et al., 2010). To date, to our knowledge, no conclusive evidence exists to implicate PI3Kβ or any other class I PI3K in the genesis of hematological malignancies such as T-ALL.

Our results demonstrate that in the absence of physiological regulation, the activity of either PI3Kγ or PI3Kδ is sufficient for the malignant transformation of T cell progenitors in a living animal. This is exemplified by the similar onset of disease and percent survival of mice lacking either p110γ or p110δ, and the rare incidence of tumor development in their combined absence. Moreover, pharmacological blockade of both p110γ and p110δ

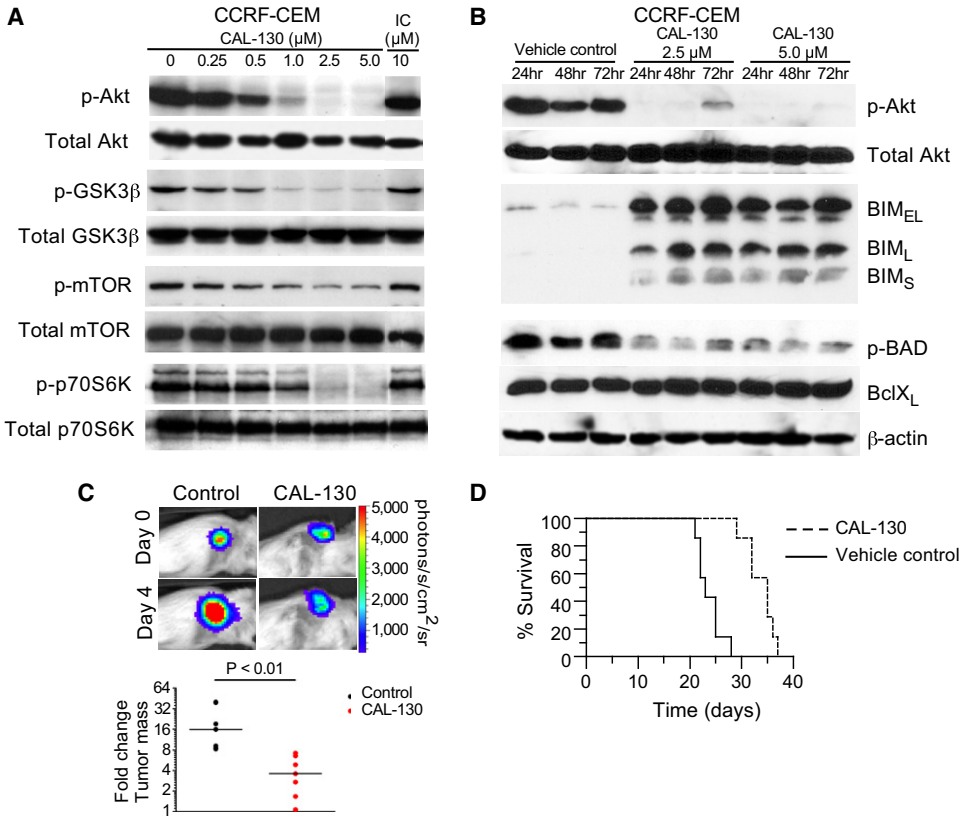

Figure 6. Effect of CAL-130 on Signaling Pathways Downstream of PI3Kγ and PI3Kδ

(A) Representative immunoblots of lysates obtained from CCRF-CEM cells treated (6 hr) with either CAL-130 or vehicle control and probed with the stated antibodies. The PI3Kδ-specific inhibitor IC87114 (IC) is shown for comparison.

(B) Representative immunoblots demonstrating activation of the proapoptotic pathway in CAL-130-treated CCRF-CEM cells.

(C) Representative bioluminescence images (upper panel) and quantification of tumor mass changes (lower panel) in mice with subcutaneous CCRF-CEM xenografts that received vehicle control or CAL-130 for 4 days (n = 7).

(D) Kaplan-Meyer analysis of overall survival of mice treated with vehicle control or CAL-130 for 7 days in a systemic CCRF-CEM xenograft model ($p < 0.01$ for CAL-130 treated versus vehicle control; n = 7 per group).

dramatically impacted on tumor cell proliferation and survival as demonstrated in CAL-130 treatment of diseased *Lck/Pten*$^{fl/fl}$ mice, IC87114 treatment of diseased *Lck/PTEN*$^{fl/fl}$;*Pik3cg*$^{-/-}$ mice, as well as CAL-130 treatment of PTEN null human T-ALL primary tumors or tumor cell lines; no such effects were observed with siRNA knockdown of either p110α or p110β, and selective blockade of PI3Kδ with IC87114 was ineffective in reducing the viability of primary human T-ALL samples. These results would suggest that propagation of upstream signaling pathways critical for the development and/or survival of PTEN null T-ALL tumors relies on PI3Kγ and PI3Kδ and that the remaining isoforms (i.e., α and β) cannot adequately compensate for their inactivity. Clearly, the same PI3K isoforms can participate in both tumorigenesis and tumor maintenance.

It has previously been established that PTEN loss is necessary but not sufficient to cause the malignant transformation of T cell progenitors (Liu et al., 2010; Guo et al., 2011). This typically requires additional genetic events such as chromosomal translocations involving the TCR α/δ locus and c-*myc* oncogene (Bernard et al., 1988; Finger et al., 1986), which are acquired during the transition from CD4$^-$CD8$^-$ DN to CD4$^+$CD8$^+$ DP development stage. Despite the presence of these strong oncogenic signals, the combined absence of PI3Kγ and PI3Kδ significantly impaired leukemogenesis, suggesting that loss of these isoforms can act as a tumorigenic bottleneck. Although it is possible that the overall reduction in CD4$^+$CD8$^+$ DP thymocyte numbers can partially account for the lower tumor incidence, we have previously shown that the transition from DN to DP thymocyte population in double-knockout mice is relatively normal (Swat et al., 2006). That is to say, there is no major deficiency in the number of early T cell progenitors that could undergo malignant transformation in the absence of PTEN activity. Yet, not only is tumorigenesis disrupted in TKO mice, but the abnormality observed in T cell development persisted as well. This is in contrast to the severe defect in thymocyte development associated with a genetic deletion of phosphoinositide-dependent kinase 1 (PDK1) (Hinton et al., 2004), a direct downstream target of class I PI3K, which can be overcome by the loss of PTEN resulting in near-normal numbers of thymocytes and peripheral T cells (Finlay et al., 2009). Similarly, PTEN deficiency can bypass a defect in either IL-7R or pre-TCR signaling, which are critical for the normal development and survival of T cells (Hagenbeek et al.,

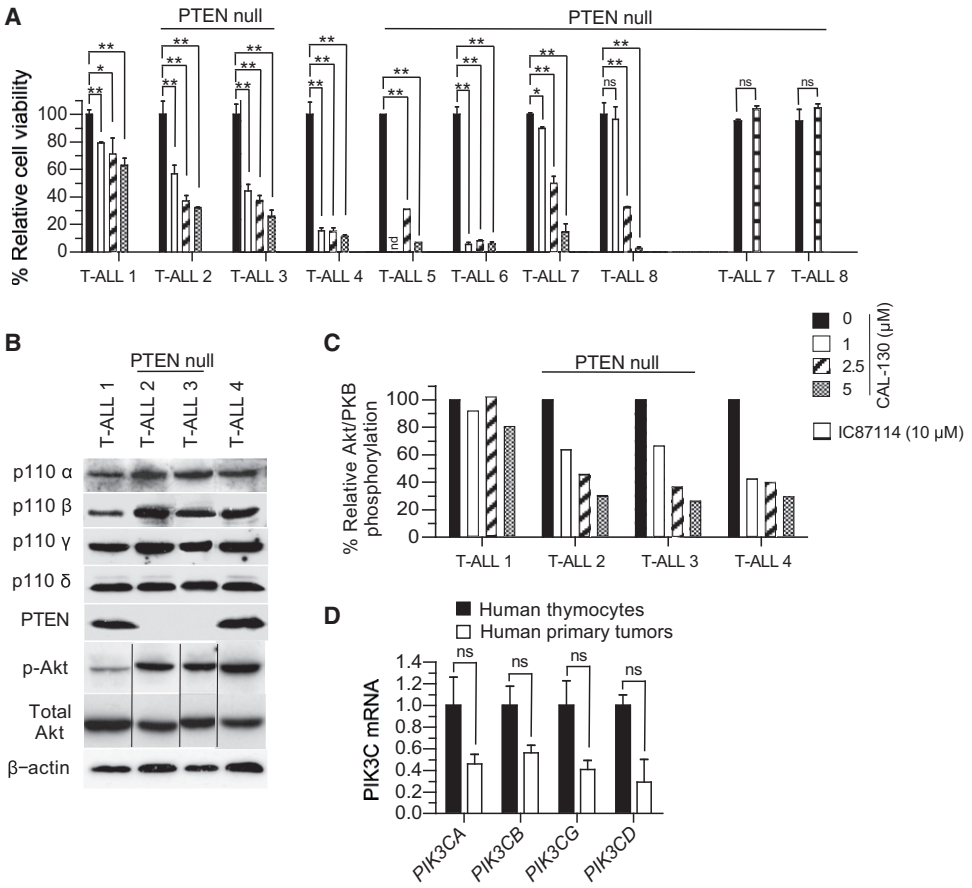

Figure 7. Susceptibility of Primary Human T-ALL Tumor Cells to Combined Inhibition of p110γ and p110δ

(A) Cell survival analyses of tumors cultured in the presence of increasing concentrations of CAL-130 for 72 hr. Percent viability indicates the proportion of live-gated cells in the treated populations relative to its vehicle control counterpart. Data represent the mean ± SD of experiments performed in duplicate or triplicate. *$p < 0.01$, **$p < 0.001$ for CAL-130 treated versus DMSO control. nd, not done; ns, not significant.

(B) Representative immunoblots of four primary human T-ALL samples to assess for expression of p110 catalytic domains and PTEN as well as phosphorylation state of Akt.

(C) Effect of CAL-130 on Akt phosphorylation on the same four representative T-ALL samples after 6 hr of treatment. Densitometry was performed on bands from immunoblots. The P-Akt signal was normalized to total Akt.

(D) Quantitative reverse-transcription PCR analysis of *PIK3C* (*A*/*B*/*G*/*D*) transcript levels in human thymocytes (n = 5) and primary human T-ALL tumors (n = 5). Error bars represent ±SD. The difference in *PIK3C* expression levels between the thymocytes and tumor cells was not statistically significant ($p > 0.05$) using a Student's t test.

2004). In stark contrast to these studies is the inability of a PTEN-deficient state to promote thymocyte proliferation and development in TKO mice. Taken together, these observations further suggest that developmental and genomic events responsible for the generation as well as the malignant transformation of T cells in the context of a PTEN-deficient state are critically reliant on proliferation and survival signals provided by PI3Kγ and PI3Kδ.

It is interesting to note that although PTEN appears to play a key role in regulating the activities of class I PI3K, it is not the only phosphatase in T cells. SHIP1 (SH2-containing inositol-5′-phosphatase) is also capable of hydrolyzing PIP3 and has been shown to play an important role in the immunoregulatory capacity and development of specific subsets of T cells (Tarasenko et al., 2007; Collazo et al., 2009). Although deletion of SHIP1 alone in T cell progenitors is not sufficient to induce leukemogenesis, low levels of this phosphatase in conjunction with PTEN inactivation have been reported in human T-ALL tumors suggesting that inactivation of both phosphatases contribute to the hyperactivation of the PI3K/Akt signaling pathway (Lo et al., 2009). Our discovery that both PI3Kγ and PI3Kδ are the engines that help drive the oncogenic process in T cell progenitors in the absence of appropriate regulation and can provide sufficient growth and survival signals necessary for tumor cell maintenance makes them attractive targets for therapy in such clinical cases. Moreover, dual inhibition of PI3Kγ and PI3Kδ in combination with conventional chemotherapies such as glucocorticoids may be of particular clinical utility in such individuals because they are more likely to fail induction chemotherapy and relapse (Gutierrez et al., 2009; Jotta et al., 2010).

It has been suggested that a complex signaling network involving PI3K exists between leukemic and supporting cells in

the tissue microenvironment that may contribute to disease progression and drug resistance (Ayala et al., 2009; Konopleva et al., 2009; Burger et al., 2009). This is exemplified by the recent observations that the PI3Kδ-specific inhibitor CAL-101 reduces levels of circulating chemokines known to contribute to tissue localization of chronic lymphocytic leukemic cells (Hoellenriegel et al., 2011). Consequently, this results in a generalized lymphocytosis during treatment of patients with this hematological malignancy. In contrast we have observed a dramatic and sustained reduction in peripheral blood T-ALL cells within hours of CAL-130 treatment of diseased *Lck/Pten*$^{fl/fl}$ mice (data not shown). That said, it is possible that paracrine and/or autocrine signaling responsible for T-ALL survival in tissues may be disrupted by simultaneously blocking the activities of PI3Kγ and PI3Kδ. Further work will be required to establish the role of these PI3K isoforms in supporting microenvironmental interactions in T-ALL.

In the broader perspective our results indicate that in the absence of PTEN-mediated regulation, distinct class I PI3K can predominate in the development and survival of tumors in a manner that is most likely to involve isoforms that normally play a critical role in the function of that particular cell type. Furthermore, we demonstrate that it is possible to target cancer cells by exploiting their "addiction" to the activity of distinct PI3K isoforms that are not themselves classical oncogenes. More generally, by identifying PI3Kγ and PI3Kδ as key therapeutic targets, it may be possible to limit toxicities that would be associated with the administration of pan-PI3K or Akt inhibitors including perturbations in insulin signaling and glucose metabolism (Crouthamel et al., 2009).

EXPERIMENTAL PROCEDURES

Cell Lines and Reagents and Antibodies

CCRF-CEM, CEM/C1, and MOLT-4 cells were obtained from ATCC and grown in RPMI-1640 medium containing 10% FBS and antibiotics. Antibodies to Akt (catalog #9272), phospho-Akt (S473, clone 193H12), phospho-mTOR (S2448, catalog #2971S), mTOR (catalog #2972), phospho-GSK3α/β (S21/9, catalog #9331S), GSK-3β (clone 27C10), phospho-p70S6K (Thr389, catalog #9205S), p70S6K (catalog #9202), and β-actin (catalog #4967S) were from Cell Signaling Technology. Antibodies to class I PI3K subunits were as follows: p110α (catalog #4255) from Cell Signaling Technology; p110β (clone Y384) from Millipore and mouse p110β from Santa Cruz Biotechnology (catalog #sc-602); p110γ (clone H1) from Jena Biosciences; and p110δ (clone H-219) from Santa Cruz Biotechnology. Antibodies to PTEN (clone 6H2.1) were from Cascade Bioscience. For flow cytometry, antibodies were obtained from BD Biosciences: CD3ε-Alexa 488 (clone 145-2C11), CD4-APC (clone RM4-5), CD8-PerCP-Cy5.5 (clone 53-6.7), CD90.2-APC (Thy-1.2, clone 53-2.1), Ki67-FITC (clone B56), and Annexin V-APC. Antibodies to Bim, phospho-Bad, Bad, and BclX_L were from Cell Signaling Technology (proapoptotic sampler kit #9942S).

The shRNA construct for p110γ in the pLKO.1 vector was obtained from Sigma-Aldrich (MISSION shRNA Plasmid DNA; clone ID: NM_002649.2-4744s1c1; TRC number: TRCN0000196870). siRNA constructs for p110α (ON-TARGET plus SMARTpool #L-003018-00) and p110β (ON-TARGET plus SMARTpool # L-003019-00) were obtained from Dharmacon (Thermo Scientific).

Primary Leukemia Samples

Cryopreserved samples were provided by collaborating institutions in the United States (Department of Pediatrics, Columbia Presbyterian Hospital and Departments of Medicine and Pathology, Vanderbilt University), The Netherlands (Erasmus MC-Sophia Children's Hospital), and Italy (Hemato-Oncology Laboratory, Department of Pediatrics, University of Padua). All samples were collected with informed consent and under the supervision of the Medical Ethics Committee of the Erasmus Medical Center, the Columbia University Medical Center Institutional Review Board, the Vanderbilt University Medical Center Institutional Review Board, and the Acute Lymphoblastic Leukemia Strategic Scientific Committee.

Cell Counts, Cell Proliferation, and Cell Viability Assay

Cell counts for mice thymi were determined as previously described by Swat et al. (2006). Cell proliferation of CCRF-CEM cells or shRNA-transfected CCRF-CEM cells, in presence or absence of appropriate drug, was followed by cell counting of samples in triplicate using a hemocytometer and trypan blue. For apoptosis determinations of untransfected or shRNA-transfected CCRF-CEMs, cells were stained with APC-conjugated Annexin-V (BD Biosciences) in Annexin Binding Buffer (Miltyeni Biotec) and analyzed by flow cytometry. For primary T-ALL samples, cell viability was assessed using the BD Cell Viability kit (BD Biosciences) coupled with the use of fluorescent-counting beads as previously described by Armstrong et al. (2009). For this, cells were plated with MS5-DL1 stroma cells, and after 72 hr following drug treatment, cells were harvested and stained with an APC-conjugated anti-human CD45 followed by a staining with the aforementioned kit according to the manufacturer's instructions.

CAL130 IC_{50}

CAL-130 is a derivative of IC87114, the synthesis of which has been previously described by Sadhu et al. (2003). IC_{50} values for CAL-130 inhibition of PI3K isoforms were determined in ex vivo PI3 kinase assays using recombinant PI3K. A ten-point kinase inhibitory profile was determined with ATP at a concentration consistent with the K_M for each enzyme (Puri et al., 2004).

Calcium Flux Measurements in Thymocytes

Ca^{2+} flux measurements in single-cell suspensions of mouse thymocytes were performed as previously described by Swat et al. (2006). Drug inhibition of Ca^{2+} flux was measured after 30 min preincubation with CAL-130 at room temperature of dye-loaded cells. Percent overall change in Ca^{2+} flux is reported as $(Ca^{2+}\ flux_{peak} - Ca^{2+}\ flux_{baseline}/Ca^{2+}flux_{ionomycin} - Ca^{2+}\ flux_{baseline}) \times 100$.

Flow Cytometry for Cell Surface Staining and Apoptosis

For cell surface staining in mouse whole blood, following incubation with appropriate antibodies, blood was processed using the BD Bioscience BD FACS Lysing Solution according to the manufacturer's instructions. For intracellular staining of Ki67, immediately after RBC lysis with the BD FACS Lysing solution, cells were permeabilized without washing with 0.025% Tween 20 in lysing solution for an additional 15 min, washed, and then incubated with Ki67 antibodies. For thymocytes, single-cell suspensions of thymocytes were isolated and stained with the appropriate antibodies as previously described by Swat et al. (2006).

Histological and Immunohistochemical Study of Tissue Samples

Formalin-fixed paraffin-embedded 5 μm tissue sections were stained with hematoxylin and eosin for histopathological diagnosis. For immunohistochemistry we performed anti-CD3 (rabbit polyclonal; Dako) staining on tissue sections after antigen retrieval by microwave heating in citrate buffer (pH 6.0). After epitope recovery, slides were incubated with antibody (anti-CD3 1:50) overnight at room temperature before antigen detection with diaminobenzidine (DAB) using a Ventana automated staining platform (Ventana).

Western Blotting

Cell lysates (from cell lines or thymocytes) were prepared on ice in M-PER Mammalian Protein Extraction reagent (Pierce) containing a cocktail of protease and phosphatase inhibitors as previously described by Swat et al. (2006). Equal amounts of total protein from lysates were subjected to SDS-PAGE, transferred to PVDF membrane (Immobilon-P; Millipore), and membranes were probed by overnight incubation with appropriate primary antibodies. Bound antibodies were visualized with HRP-conjugated secondary antibodies and ECL chemistry (SuperPico West; Pierce).

shRNA and siRNA Knockdown

CCRF-CEMs were transfected using the Amaxa Human T cell Nucleofecor kit (Lonza) according to the manufacturer's optimized protocol kit for this cell line. For shRNA knockdown of p110γ, CCRF-CEMs (2×10^6 cells) were transfected with 2 μg of purified plasmid DNA, and clones were selected by high dilution in puromycin used at a concentration predetermined by a killing curve. Expression of p110γ and p110δ was determined by western blotting.

For siRNA knockdown of p110α or p110β, CCRF-CEMs (2×10^6 cells) were transfected with 300 nM of siRNA construct. After a brief recovery period, cells were diluted to between 1 and 2×10^5/ml and grown for further 48 hr for cell counting, flow cytometry, and western blotting.

Mice and Animal Procedures

All mice were kept in a specific pathogen-free facility at Columbia University Medical Center. All mice studies and breeding were carried out under the approval of Institutional Animal Care and Use Committee of Columbia University. NOD.Cg-*Prkdc*^{scid} *Il2rg*^{tm1Wjl}/Sz mice for xenograft experiments and *Gt(ROSA)26Sor*$^{tm1(Luc)Kael}$/J for bioimaging studies were obtained from The Jackson Laboratory. Mice deficient for *Pten* in the T cell lineage were generated by crossing *Lck-cre* with floxed *Pten* (Hennet et al., 1995; Trotman et al., 2003). P110γ$^{-/-}$ and p110δ$^{-/-}$ mice have been previously described by Swat et al. (2006). These animals were intercrossed with *Lck-cre/Pten*$^{fl/fl}$ animals to generate mice homozygous mutant for either p110γ or p110δ and *Pten* or homozygous mutant for p110γ, 110δ, and *Pten*.

For subcutaneous xenograft experiments, luminescent CCRF-CEM (CEM-luc) cells were generated by lentiviral infection with FUW-luc and selection with neomycin. Luciferase expression was verified with the Dual-Luciferase Reporter Assay kit (Promega). We injected 2.5×10^6 CEM-luc cells embedded in Matrigel (BD Biosciences) in the flank of NOD.Cg-*Prkdc*^{scid} *Il2rg*^{tm1Wjl}/Sz mice. After 1 week, mice were treated by oral gavage with vehicle (0.5% methyl cellulose, 0.1% Tween 80), or CAL-130 (10 mg kg^{-1}) every 8 hr daily for 4 days, and then tumors were imaged as follows: mice anesthetized by isoflurane inhalation were injected intraperitoneally with D-luciferin (50 mg kg^{-1}; Xenogen). Photonic emission was imaged with the In Vivo Imaging System (IVIS; Xenogen). Tumor bioluminescence was quantified by integrating the photonic flux (photons per second) through a region encircling each tumor using the Living Image software package (Xenogen). Administration of D-luciferin and detection of tumor bioluminescence in *Lck/Pten*$^{fl/fl}$*/Gt(ROSA)26Sor*$^{tm1(Luc)Kael}$/J mice were performed in a similar manner.

For intravenous xenograft transplantation, 5×10^6 CCRF-CEM cells were injected intravenously in 14 NOD.Cg-*Prkdc*^{scid} *Il2rg*^{tm1Wjl}/Sz mice. After 3 days, mice were segregated into two treatment groups that received either CAL-130 or vehicle by oral gavage as described above for 7 days. Mice in both groups were then followed until moribund (and euthanized).

Plasma Levels of CAL130, Glucose, and Insulin

For CAL-130 level determinations, animals received a single oral dose (10 or 20 mg kg^{-1}) of inhibitor. Plasma was collected at 0, 2, 4, 8, and 12 hr and subjected to high-performance liquid chromatography-MS/MS (sensitivity 1 ng/ml). The concentration of CAL-130 in plasma was determined using a standard curve (analyte peak area versus concentration) generated with calibration standard pools. Values represent the mean (±SD) for four animals per group.

Plasma glucose and insulin levels were determined following a single oral dose of CAL-130 (10 mg kg^{-1}). Blood was collected into K_2EDTA tubes by cardiac puncture at baseline and 0, 2, 4, and 8 hr post-dose, and plasma samples were frozen at −80°C until analysis. The insulin and glucose levels were determined by using an Ultra Sensitive Mouse Insulin ELISA Kit (Crystal Chem) or WaveSense Presto Blood Glucose Monitoring System (Agamatrix, Boston), respectively.

Statistical Analyses

Statistical analyses were performed using Student's t test (GraphPad Prism software). Kaplan-Meier survival curves were analyzed using a log rank test (GraphPad Prism software). Values were considered significant at $p < 0.05$.

SUPPLEMENTAL INFORMATION

Supplemental Information includes three figures, one table, and Supplemental Experimental Procedures and can be found with this article online at doi:10.1016/j.ccr.2012.02.029.

ACKNOWLEDGMENTS

We thank Andrew Kung for providing the FUW luciferase vector, Jerry Evarts for supplying CAL-130, Juan Carlos Zuniga-Pflucker for providing the OP9-DL1 cells, Richard Friedman for statistical analyses, Kui Tan and Mikin Patel for genotyping and animal husbandry, and Timothy Wang for critical review of the manuscript. This work was supported by the DOD (Grant PR093714 to T.G.D. and A.F.), the Leukemia & Lymphoma Society Translational Research Program (Grant 140229 to T.G.D. and A.F.), and the Leukemia & Lymphoma Society Scholar Award (to A.F.). B.J.L. and A.K. are employees of the company (Gilead Sciences) that manufactured CAL-130.

Received: August 10, 2011
Revised: December 26, 2011
Accepted: February 24, 2012
Published: April 16, 2012

REFERENCES

Armstrong, F., Brunet de la Grange, P., Gerby, B., Rouyez, M.C., Calvo, J., Fontenay, M., Boissel, N., Dombret, H., Baruchel, A., Landman-Parker, J., et al. (2009). NOTCH is a key regulator of human T-cell acute leukemia initiating cell activity. Blood *113*, 1730–1740.

Ayala, F., Dewar, R., Kieran, M., and Kalluri, R. (2009). Contribution of bone microenvironment to leukemogenesis and leukemia progression. Leukemia *23*, 2233–2241.

Beesley, A.H., Firth, M.J., Ford, J., Weller, R.E., Freitas, J.R., Perera, K.U., and Kees, U.R. (2009). Glucocorticoid resistance in T-lineage acute lymphoblastic leukaemia is associated with a proliferative metabolism. Br. J. Cancer *100*, 1926–1936.

Bernard, O., Larsen, C.J., Hampe, A., Mauchauffé, M., Berger, R., and Mathieu-Mahul, D. (1988). Molecular mechanisms of a t(8;14)(q24;q11) translocation juxtaposing c-myc and TcR-alpha genes in a T-cell leukaemia: involvement of a V alpha internal heptamer. Oncogene *2*, 195–200.

Burger, J.A., Ghia, P., Rosenwald, A., and Caligaris-Cappio, F. (2009). The microenvironment in mature B-cell malignancies: a target for new treatment strategies. Blood *114*, 3367–3375.

Cantley, L.C. (2002). The phosphoinositide 3-kinase pathway. Science *296*, 1655–1657.

Carnero, A., Blanco-Aparicio, C., Renner, O., Link, W., and Leal, J.F. (2008). The PTEN/PI3K/AKT signalling pathway in cancer, therapeutic implications. Curr. Cancer Drug Targets *8*, 187–198.

Cohen, P., and Frame, S. (2001). The renaissance of GSK3. Nat. Rev. Mol. Cell Biol. *2*, 769–776.

Collazo, M.M., Wood, D., Paraiso, K.H., Lund, E., Engelman, R.W., Le, C.T., Stauch, D., Kotsch, K., and Kerr, W.G. (2009). SHIP limits immunoregulatory capacity in the T-cell compartment. Blood *113*, 2934–2944.

Crouthamel, M.C., Kahana, J.A., Korenchuk, S., Zhang, S.Y., Sundaresan, G., Eberwein, D.J., Brown, K.K., and Kumar, R. (2009). Mechanism and management of AKT inhibitor-induced hyperglycemia. Clin. Cancer Res. *15*, 217–225.

Duronio, V. (2008). The life of a cell: apoptosis regulation by the PI3K/PKB pathway. Biochem. J. *415*, 333–344.

Erlacher, M., Michalak, E.M., Kelly, P.N., Labi, V., Niederegger, H., Coultas, L., Adams, J.M., Strasser, A., and Villunger, A. (2005). BH3-only proteins Puma and Bim are rate-limiting for gamma-radiation- and glucocorticoid-induced apoptosis of lymphoid cells in vivo. Blood *106*, 4131–4138.

Fabian, M.A., Biggs, W.H., 3rd, Treiber, D.K., Atteridge, C.E., Azimioara, M.D., Benedetti, M.G., Carter, T.A., Ciceri, P., Edeen, P.T., Floyd, M., et al. (2005). A

small molecule-kinase interaction map for clinical kinase inhibitors. Nat. Biotechnol. *23*, 329–336.

Finger, L.R., Harvey, R.C., Moore, R.C., Showe, L.C., and Croce, C.M. (1986). A common mechanism of chromosomal translocation in T- and B-cell neoplasia. Science *234*, 982–985.

Finlay, D.K., Sinclair, L.V., Feijoo, C., Waugh, C.M., Hagenbeek, T.J., Spits, H., and Cantrell, D.A. (2009). Phosphoinositide-dependent kinase 1 controls migration and malignant transformation but not cell growth and proliferation in PTEN-null lymphocytes. J. Exp. Med. *206*, 2441–2454.

Foukas, L.C., Berenjeno, I.M., Gray, A., Khwaja, A., and Vanhaesebroeck, B. (2010). Activity of any class IA PI3K isoform can sustain cell proliferation and survival. Proc. Natl. Acad. Sci. USA *107*, 11381–11386.

Guo, W., Lasky, J.L., Chang, C.J., Mosessian, S., Lewis, X., Xiao, Y., Yeh, J.E., Chen, J.Y., Iruela-Arispe, M.L., Varella-Garcia, M., and Wu, H. (2008). Multi-genetic events collaboratively contribute to Pten-null leukaemia stem-cell formation. Nature *453*, 529–533.

Guo, W., Schubbert, S., Chen, J.Y., Valamehr, B., Mosessian, S., Shi, H., Dang, N.H., Garcia, C., Theodoro, M.F., Varella-Garcia, M., and Wu, H. (2011). Suppression of leukemia development caused by PTEN loss. Proc. Natl. Acad. Sci. USA *108*, 1409–1414.

Gutierrez, A., Sanda, T., Grebliunaite, R., Carracedo, A., Salmena, L., Ahn, Y., Dahlberg, S., Neuberg, D., Moreau, L.A., Winter, S.S., et al. (2009). High frequency of PTEN, PI3K, and AKT abnormalities in T-cell acute lymphoblastic leukemia. Blood *114*, 647–650.

Hagenbeek, T.J., and Spits, H. (2008). T-cell lymphomas in T-cell-specific Pten-deficient mice originate in the thymus. Leukemia *22*, 608–619.

Hagenbeek, T.J., Naspetti, M., Malergue, F., Garçon, F., Nunès, J.A., Cleutjens, K.B., Trapman, J., Krimpenfort, P., and Spits, H. (2004). The loss of PTEN allows TCR alphabeta lineage thymocytes to bypass IL-7 and Pre-TCR-mediated signaling. J. Exp. Med. *200*, 883–894.

Hennet, T., Hagen, F.K., Tabak, L.A., and Marth, J.D. (1995). T-cell-specific deletion of a polypeptide N-acetylgalactosaminyl-transferase gene by site-directed recombination. Proc. Natl. Acad. Sci. USA *92*, 12070–12074.

Hickey, F.B., and Cotter, T.G. (2006). BCR-ABL regulates phosphatidylinositol 3-kinase-p110gamma transcription and activation and is required for proliferation and drug resistance. J. Biol. Chem. *281*, 2441–2450.

Hinton, H.J., Alessi, D.R., and Cantrell, D.A. (2004). The serine kinase phosphoinositide-dependent kinase 1 (PDK1) regulates T cell development. Nat. Immunol. *5*, 539–545.

Hoellenriegel, J., Meadows, S.A., Sivina, M., Wierda, W.G., Kantarjian, H., Keating, M.J., Giese, N., O'Brien, S., Yu, A., Miller, L.L., et al. (2011). The phosphoinositide 3′-kinase delta inhibitor, CAL-101, inhibits B-cell receptor signaling and chemokine networks in chronic lymphocytic leukemia. Blood *118*, 3603–3612.

Huang, W.C., and Hung, M.C. (2009). Induction of Akt activity by chemotherapy confers acquired resistance. J. Formos. Med. Assoc. *108*, 180–194.

Jackson, S.P., Schoenwaelder, S.M., Goncalves, I., Nesbitt, W.S., Yap, C.L., Wright, C.E., Kenche, V., Anderson, K.E., Dopheide, S.M., Yuan, Y., et al. (2005). PI 3-kinase p110beta: a new target for antithrombotic therapy. Nat. Med. *11*, 507–514.

Ji, H., Rintelen, F., Waltzinger, C., Bertschy Meier, D., Bilancio, A., Pearce, W., Hirsch, E., Wymann, M.P., Rückle, T., Camps, M., et al. (2007). Inactivation of PI3Kgamma and PI3Kdelta distorts T-cell development and causes multiple organ inflammation. Blood *110*, 2940–2947.

Jia, S., Liu, Z., Zhang, S., Liu, P., Zhang, L., Lee, S.H., Zhang, J., Signoretti, S., Loda, M., Roberts, T.M., and Zhao, J.J. (2008). Essential roles of PI(3)K-p110beta in cell growth, metabolism and tumorigenesis. Nature *454*, 776–779.

Jotta, P.Y., Ganazza, M.A., Silva, A., Viana, M.B., da Silva, M.J., Zambaldi, L.J., Barata, J.T., Brandalise, S.R., and Yunes, J.A. (2010). Negative prognostic impact of PTEN mutation in pediatric T-cell acute lymphoblastic leukemia. Leukemia *24*, 239–242.

Kang, S., Denley, A., Vanhaesebroeck, B., and Vogt, P.K. (2006). Oncogenic transformation induced by the p110beta, -gamma, and -delta isoforms of class I phosphoinositide 3-kinase. Proc. Natl. Acad. Sci. USA *103*, 1289–1294.

Karaman, M.W., Herrgard, S., Treiber, D.K., Gallant, P., Atteridge, C.E., Campbell, B.T., Chan, K.W., Ciceri, P., Davis, M.I., Edeen, P.T., et al. (2008). A quantitative analysis of kinase inhibitor selectivity. Nat. Biotechnol. *26*, 127–132.

Katso, R., Okkenhaug, K., Ahmadi, K., White, S., Timms, J., and Waterfield, M.D. (2001). Cellular function of phosphoinositide 3-kinases: implications for development, homeostasis, and cancer. Annu. Rev. Cell Dev. Biol. *17*, 615–675.

Konopleva, M., Tabe, Y., Zeng, Z., and Andreeff, M. (2009). Therapeutic targeting of microenvironmental interactions in leukemia: mechanisms and approaches. Drug Resist. Updat. *12*, 103–113.

Larson Gedman, A., Chen, Q., Kugel Desmoulin, S., Ge, Y., LaFiura, K., Haska, C.L., Cherian, C., Devidas, M., Linda, S.B., Taub, J.W., and Matherly, L.H. (2009). The impact of NOTCH1, FBW7 and PTEN mutations on prognosis and downstream signaling in pediatric T-cell acute lymphoblastic leukemia: a report from the Children's Oncology Group. Leukemia *23*, 1417–1425.

Liu, X., Karnell, J.L., Yin, B., Zhang, R., Zhang, J., Li, P., Choi, Y., Maltzman, J.S., Pear, W.S., Bassing, C.H., and Turka, L.A. (2010). Distinct roles for PTEN in prevention of T cell lymphoma and autoimmunity in mice. J. Clin. Invest. *120*, 2497–2507.

Lo, T.C., Barnhill, L.M., Kim, Y., Nakae, E.A., Yu, A.L., and Diccianni, M.B. (2009). Inactivation of SHIP1 in T-cell acute lymphoblastic leukemia due to mutation and extensive alternative splicing. Leuk. Res. *33*, 1562–1566.

Maser, R.S., Choudhury, B., Campbell, P.J., Feng, B., Wong, K.K., Protopopov, A., O'Neil, J., Gutierrez, A., Ivanova, E., Perna, I., et al. (2007). Chromosomally unstable mouse tumours have genomic alterations similar to diverse human cancers. Nature *447*, 966–971.

Okkenhaug, K., and Vanhaesebroeck, B. (2003). PI3K in lymphocyte development, differentiation and activation. Nat. Rev. Immunol. *3*, 317–330.

Palomero, T., Dominguez, M., and Ferrando, A.A. (2008). The role of the PTEN/AKT Pathway in NOTCH1-induced leukemia. Cell Cycle *7*, 965–970.

Puri, K.D., Doggett, T.A., Douangpanya, J., Hou, Y., Tino, W.T., Wilson, T., Graf, T., Clayton, E., Turner, M., Hayflick, J.S., and Diacovo, T.G. (2004). Mechanisms and implications of phosphoinositide 3-kinase δ in promoting neutrophil trafficking into inflamed tissue. Blood *103*, 3448–3456.

Sadhu, C., Masinovsky, B., Dick, K., Sowell, C.G., and Staunton, D.E. (2003). Essential role of phosphoinositide 3-kinase δ in neutrophil directional movement. J. Immunol. *170*, 2647–2654.

Safran, M., Kim, W.Y., Kung, A.L., Horner, J.W., DePinho, R.A., and Kaelin, W.G., Jr. (2003). Mouse reporter strain for noninvasive bioluminescent imaging of cells that have undergone Cre-mediated recombination. Mol. Imaging *2*, 297–302.

Salmena, L., Carracedo, A., and Pandolfi, P.P. (2008). Tenets of PTEN tumor suppression. Cell *133*, 403–414.

Samuels, Y., Wang, Z., Bardelli, A., Silliman, N., Ptak, J., Szabo, S., Yan, H., Gazdar, A., Powell, S.M., Riggins, G.J., et al. (2004). High frequency of mutations of the PIK3CA gene in human cancers. Science *304*, 554.

Schmelzle, T., and Hall, M.N. (2000). TOR, a central controller of cell growth. Cell *103*, 253–262.

Silva, A., Yunes, J.A., Cardoso, B.A., Martins, L.R., Jotta, P.Y., Abecasis, M., Nowill, A.E., Leslie, N.R., Cardoso, A.A., and Barata, J.T. (2008). PTEN posttranslational inactivation and hyperactivation of the PI3K/Akt pathway sustain primary T cell leukemia viability. J. Clin. Invest. *118*, 3762–3774.

Sopasakis, V.R., Liu, P., Suzuki, R., Kondo, T., Winnay, J., Tran, T.T., Asano, T., Smyth, G., Sajan, M.P., Farese, R.V., et al. (2010). Specific roles of the p110alpha isoform of phosphatidylinsositol 3-kinase in hepatic insulin signaling and metabolic regulation. Cell Metab. *11*, 220–230.

Strasser, A., Puthalakath, H., Bouillet, P., Huang, D.C., O'Connor, L., O'Reilly, L.A., Cullen, L., Cory, S., and Adams, J.M. (2000). The role of bim, a proapoptotic BH3-only member of the Bcl-2 family in cell-death control. Ann. N Y Acad. Sci. *917*, 541–548.

Sujobert, P., Bardet, V., Cornillet-Lefebvre, P., Hayflick, J.S., Prie, N., Verdier, F., Vanhaesebroeck, B., Muller, O., Pesce, F., Ifrah, N., et al. (2005). Essential

role for the p110delta isoform in phosphoinositide 3-kinase activation and cell proliferation in acute myeloid leukemia. Blood *106*, 1063–1066.

Sulis, M.L., and Parsons, R. (2003). PTEN: from pathology to biology. Trends Cell Biol. *13*, 478–483.

Suzuki, A., Yamaguchi, M.T., Ohteki, T., Sasaki, T., Kaisho, T., Kimura, Y., Yoshida, R., Wakeham, A., Higuchi, T., Fukumoto, M., et al. (2001). T cell-specific loss of Pten leads to defects in central and peripheral tolerance. Immunity *14*, 523–534.

Swat, W., Montgrain, V., Doggett, T.A., Douangpanya, J., Puri, K., Vermi, W., and Diacovo, T.G. (2006). Essential role of PI3Kdelta and PI3Kgamma in thymocyte survival. Blood *107*, 2415–2422.

Tarasenko, T., Kole, H.K., Chi, A.W., Mentink-Kane, M.M., Wynn, T.A., and Bolland, S. (2007). T cell-specific deletion of the inositol phosphatase SHIP reveals its role in regulating Th1/Th2 and cytotoxic responses. Proc. Natl. Acad. Sci. USA *104*, 11382–11387.

Trotman, L.C., Niki, M., Dotan, Z.A., Koutcher, J.A., Di Cristofano, A., Xiao, A., Khoo, A.S., Roy-Burman, P., Greenberg, N.M., Van Dyke, T., et al. (2003). Pten dose dictates cancer progression in the prostate. PLoS Biol. *1*, E59.

Wang, Z., Malone, M.H., He, H., McColl, K.S., and Distelhorst, C.W. (2003). Microarray analysis uncovers the induction of the proapoptotic BH3-only protein Bim in multiple models of glucocorticoid-induced apoptosis. J. Biol. Chem. *278*, 23861–23867.

Webb, L.M., Vigorito, E., Wymann, M.P., Hirsch, E., and Turner, M.J. (2005). Cutting edge: T cell development requires the combined activities of the p110gamma and p110delta catalytic isoforms of phosphatidylinositol 3-kinase. J. Immunol. *175*, 2783–2787.

Wee, S., Wiederschain, D., Maira, S.M., Loo, A., Miller, C., deBeaumont, R., Stegmeier, F., Yao, Y.M., and Lengauer, C. (2008). PTEN-deficient cancers depend on PIK3CB. Proc. Natl. Acad. Sci. USA *105*, 13057–13062.

Yuan, T.L., and Cantley, L.C. (2008). PI3K pathway alterations in cancer: variations on a theme. Oncogene *27*, 5497–5510.

Zhao, L., and Vogt, P.K. (2008). Class I PI3K in oncogenic cellular transformation. Oncogene *27*, 5486–5496.

Zunder, E.R., Knight, Z.A., Houseman, B.T., Apsel, B., and Shokat, K.M. (2008). Discovery of drug-resistant and drug-sensitizing mutations in the oncogenic PI3K isoform p110 alpha. Cancer Cell *14*, 180–192.